

Carbonyl Clusters as Homogeneous Catalysts. Kinetic and Molecular Aspects of the Hydrogenation of Diphenylacetylene Promoted by an Alkenyl-Bridged Triruthenium Cluster Complex

Javier A. Cabeza,* José M. Fernández-Colinas, Angela Llamazares, and Víctor Riera

Instituto de Química Organometálica, Facultad de Química, Universidad de Oviedo, 33071 Oviedo, Spain

Santiago García-Granda and Juan F. Van der Maelen

Departamento de Química Física y Analítica, Universidad de Oviedo, 33071 Oviedo, Spain

Received May 18, 1994[®]

The cluster complex $[\text{Ru}_3(\mu_3\text{-ampy})(\mu\text{-}\eta^1\text{:}\eta^2\text{-PhC=CHPh})(\text{CO})_8]$ (**1**; Humpy = 2-amino-6-methylpyridine), which contains a bridging alkenyl ligand, promotes the selective homogeneous hydrogenation of diphenylacetylene to *cis*- and *trans*-stilbene under very mild conditions (333 K, $P(\text{H}_2) < 1$ atm). Compound **1** is the only metal complex observed by IR spectroscopy in the catalytic solution. This complex reacts with hydrogen at room temperature, in the absence of diphenylacetylene, to give a mixture of *cis*- and *trans*-stilbene and the known cluster compounds $[\text{Ru}_3(\mu\text{-H})(\mu_3\text{-ampy})(\text{CO})_9]$ (**2**) and $[\text{Ru}_6(\mu\text{-H})_6(\mu_3\text{-ampy})_2(\text{CO})_{14}]$ (**3**); however, these products are not observed in the presence of diphenylacetylene. The reaction of **1** with carbon monoxide gives the nonacarbonyl derivative $[\text{Ru}_3(\mu_3\text{-ampy})(\eta^1\text{-PhC=CHPh})(\text{CO})_9]$ (**4**), which contains a terminal alkenyl ligand. Reaction of complex **1** with $\text{HBF}_4\cdot\text{OEt}_2$ gives the cationic compound $[\text{Ru}_3(\mu\text{-H})(\mu_3\text{-ampy})(\mu\text{-}\eta^1\text{:}\eta^2\text{-PhC=CHPh})(\text{CO})_8][\text{BF}_4]$ (**5**), which has been crystallographically characterized. Crystal data for **5**· CH_2Cl_2 : triclinic, space group $P\bar{1}$, $a = 10.357(9)$ Å, $b = 11.279(5)$ Å, $c = 16.751(9)$ Å, $\alpha = 105.42(6)^\circ$, $\beta = 97.68(6)^\circ$, $\gamma = 100.61(4)^\circ$, $Z = 2$. Complex **5** reacts with $[\text{PPN}][\text{BH}_4]$ to give *cis*- and *trans*-stilbene as well as a coordinatively unsaturated derivative which on exposure to diphenylacetylene regenerates complex **1**. These results, coupled with a kinetic study of the catalytic hydrogenation reaction, which is first order in cluster and hydrogen concentrations and negative or zero order (depending on the [substrate]:[catalyst] ratio) in diphenylacetylene concentration, support a hydrogenation mechanism. This mechanism corresponds to the general rate law $-\text{d}[\text{Ph}_2\text{C}_2]/\text{d}t = \{k_a + k_b[\text{Ph}_2\text{C}_2]^{-1}\} [\text{1}] (P(\text{H}_2))$, in which the catalytic species are trinuclear, and consists of two coupled catalytic cycles, one working preferably at $[\text{Ph}_2\text{C}_2]:[\text{1}] < 50$ and the other at $[\text{Ph}_2\text{C}_2]:[\text{1}] > 50$.

Introduction

Although many mechanisms of homogeneous reactions catalyzed by mononuclear transition-metal complexes are now well-known,¹ only a few mechanisms of homogeneous reactions catalyzed by transition-metal cluster compounds have been determined.²

Efforts have been devoted to establish whether or not a catalyst precursor changes its nuclearity during a

cluster-promoted catalytic reaction,^{2,3} and in this context, as far as hydrogenation reactions with ruthenium cluster complexes as catalyst precursors are concerned, the presence of polynuclear catalytic species has been confirmed only in a few instances;²⁻⁵ in other cases, the precursor fragments under the catalytic conditions give rise to species of different nuclearity,^{2,3,6,7} whereas in most cases, the fate of the catalytic precursor is unknown.^{2,8-11} However, knowledge of the catalyst nuclearity is only a small step toward finding the

[®] Abstract published in *Advance ACS Abstracts*, October 1, 1994.

(1) See, for example: (a) Parshall, G. W.; Ittel, S. D. *Homogeneous Catalysis: The Applications and Chemistry of Catalysis by Soluble Transition-Metal Complexes*; Wiley: New York, 1992. (b) Masters, C. *Homogeneous Transition-Metal Catalysis*; Chapman and Hall: London, 1981. (c) Halpern, J. *Pure Appl. Chem.* **1987**, *59*, 173. (d) Sánchez-Delgado, R. A.; Rondón, D.; Andriollo, A.; Herrera, V.; Martín, G.; Chaudret, B. *Organometallics* **1993**, *12*, 4291 and references therein. (e) Esteruelas, M. A.; López, A. M.; Oro, L. A.; Pérez, A.; Schulz, M.; Werner, H. *Organometallics* **1993**, *12*, 1823. (f) Esteruelas, M. A.; Oro, L. A.; Valero, C. *Organometallics* **1992**, *11*, 3362.

(2) For relevant reviews on metal clusters in homogeneous catalysis, see: (a) Gladfelter, W. L.; Roessellet, K. J. In *The Chemistry of Metal Cluster Complexes*; Shriver, D. F., Kaesz, H. D., Adams, R. D., Eds.; VCH: New York, 1990; Chapter 7, p 329. (b) Süß-Fink, G.; Meister, G. *Adv. Organomet. Chem.* **1993**, *35*, 41.

(3) See, for example: (a) Lewis, L. N. *Chem. Rev.* **1993**, *93*, 2693 and references therein. (b) Laine, R. M. *J. Mol. Catal.* **1982**, *14*, 137.

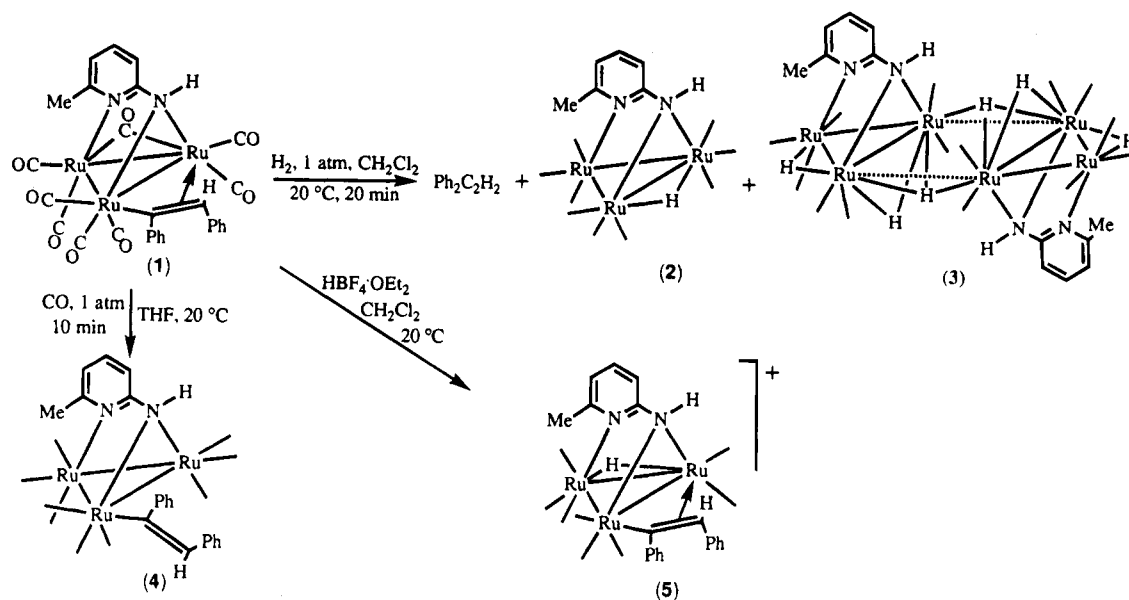
(4) (a) Doi, Y.; Koshizuka, K.; Keii, T. *Inorg. Chem.* **1982**, *21*, 2732. (b) Doi, Y.; Tamura, S.; Koshizuka, K. *J. Mol. Catal.* **1983**, *19*, 213. (c) Smieja, J. A.; Gozum, J. E.; Gladfelter, W. L. *Organometallics* **1986**, *5*, 2154. (d) Zuffa, J. L.; Blohm, M. L.; Gladfelter, W. L. *J. Am. Chem. Soc.* **1986**, *108*, 552.

(5) Cabeza, J. A.; Fernández-Colinas, J. M.; Llamazares, A.; Riera, V. *Organometallics* **1993**, *12*, 4141.

(6) Cabeza, J. A.; Fernández-Colinas, J. M.; Llamazares, A.; Riera, V. *Organometallics* **1992**, *11*, 4355.

(7) See, for example: (a) Knifton, J. F. *J. Am. Chem. Soc.* **1981**, *103*, 3959. (b) Warren, B. K.; Dombek, B. D. *J. Catal.* **1983**, *79*, 334. (c) Mercer, G. D.; Shing-Shu, J.; Brauchfuss, T. B.; Roundhill, D. M. *J. Am. Chem. Soc.* **1975**, *97*, 1967. (d) Sánchez-Delgado, R.; Andriollo, A.; Puga, J.; Martín, G. *Inorg. Chem.* **1987**, *26*, 1867.

Scheme 1



mechanism of a cluster-promoted catalytic reaction. Kinetic, chemical, and spectroscopic studies are essential when one attempts to characterize any catalytic species.

We now report the catalytic activity of the alkenyl-bridged cluster complex $[Ru_3(\mu_3\text{-ampy})(\mu\text{-}\eta^1\text{:}\eta^2\text{-PhC=CHPh})(CO)_8]$ (1) (Hampy = 2-amino-6-methylpyridine) (Scheme 1)¹² in the homogeneous hydrogenation of diphenylacetylene. We also describe relevant chemical, kinetic, and spectroscopic studies that support a hydrogenation mechanism in which only trinuclear cluster species are involved.

Experimental Section

General Data. Solvents were dried over sodium benzophenone ketyl (THF, diethyl ether, hydrocarbons) or CaH_2 (dichlo-

romethane) and distilled under nitrogen prior to use. Unless otherwise stated, the reactions were carried out under nitrogen at room temperature, using Schlenk–vacuum-line techniques, and were routinely monitored by solution IR spectroscopy (carbonyl stretching region). Compounds 1,¹⁰ 2,¹³ and 3¹¹ were prepared as described previously. All other reagents were used as received from Aldrich. Plates for qualitative TLC analyses (silica gel) were also purchased from Aldrich. Infrared spectra were recorded on a Perkin-Elmer FT 1720-X spectrophotometer, using 0.1-mm CaF_2 cells. 1H and ^{13}C DEPT NMR spectra were run at 23 °C with Bruker AC-200 and AC-300 instruments, using $SiMe_4$ as internal standard (δ 0 ppm). Microanalyses were obtained from the University of Oviedo Analytical Service. GC analyses were carried out at 175 °C on a Perkin-Elmer 8600 gas chromatograph, equipped with a 12-m AQ2 capillary column (i.d. 0.22 mm) and a flame ionization detector; quantification was achieved with a PE-Nelson 1020 integrator. Plots of the kinetic data were fitted using conventional regression programs. All calculations needed for the X-ray diffraction study were performed on a Micro VAX-3400 computer at the Centro de Cálculo Científico of the University of Oviedo.

Catalytic Hydrogenation of Diphenylacetylene. The appropriate amounts of complex 1 and diphenylacetylene (Table 1) were placed in a two-necked 25-mL flask with one neck connected to a gas buret, which in turn was connected to a vacuum line. The flask was closed by a silicone septum and the system evacuated and filled with hydrogen five times. Degassed toluene (8 mL) was then introduced into the flask and the required pressure adjusted in the gas buret. The flask was immersed in a bath thermostated at 333 K and shaken during the run at 600 shakes min^{-1} with a Selecta shaker. An equilibration time of 2 min was allowed before acquiring any data. The working partial pressure of hydrogen was determined by subtracting the toluene vapor pressure at 333 K from the measured total pressure. The evolution of the catalytic reactions was followed by GC. Reaction rates were obtained by measuring the hydrogen consumption in the gas buret as a function of time.

Reaction of $[Ru_3(\mu_3\text{-ampy})(\mu\text{-}\eta^1\text{:}\eta^2\text{-PhC=CHPh})(CO)_8]$ (1) with Hydrogen. Hydrogen was bubbled through a dichloromethane solution (10 mL) of complex 1 (60 mg, 0.074 mmol) for 20 min. A GC analysis of the solution showed *cis*- and *trans*-stilbene as the only organic products, whereas IR spectroscopy and a qualitative TLC analysis revealed the

(8) (a) Markó, L.; Vici-Orosz, A. In *Metal Clusters in Catalysis*; Knözinger, H., Gates, B. C., Guczi, L., Eds.; Elsevier: Amsterdam, 1986; Chapter 5, p 89. (b) Whyman, R. In *Transition Metal Clusters*; Johnson, B. F. G., Ed.; Wiley: New York, 1980; Chapter 8, p 545.

(9) For the homogeneous hydrogenation of internal alkynes promoted by ruthenium carbonyl cluster complexes see, for example: (a) Castiglioni, M.; Giordano, R.; Sappa, E. *J. Organomet. Chem.* **1989**, *362*, 339. (b) Castiglioni, M.; Giordano, R.; Sappa, E. *J. Organomet. Chem.* **1991**, *407*, 377. (c) Michelin-Lausarot, P.; Vaglio, G. A.; Valle, M. *Inorg. Chim. Acta* **1977**, *25*, L107. (d) Michelin-Lausarot, P.; Vaglio, G. A.; Valle, M. *Inorg. Chim. Acta* **1979**, *36*, 213. (e) Lugan, N.; Laurent, F.; Lavigne, G.; Newcomb, T. P.; Liimata, E. W.; Bonnet, J.-J. *J. Am. Chem. Soc.* **1990**, *112*, 8607.

(10) Cabeza, J. A.; Fernández-Colinas, J. M.; Llamazares, A.; Riera, V. *J. Mol. Catal.* **1992**, *71*, L7.

(11) Cabeza, J. A.; Fernández-Colinas, J. M.; García-Granda, S.; Llamazares, A.; López-Ortiz, F.; Riera, V.; Van der Maelen, J. F. *Organometallics* **1994**, *13*, 426.

(12) The structure proposed for complex 1 in previous works,^{10,12a,b} in which the alkenyl ligand spans one of the two Ru–Ru edges unbridged by the amido fragment of the ampy ligand and which was based on the X-ray structure of $[Ru_3(\mu_3\text{-ampy})(\mu\text{-}\eta^1\text{:}\eta^2\text{-PhC=CHPh})(CO)_8]$ (Hampy = 2-anilino-6-methylpyridine),^{9e} differs slightly from that proposed in this paper for the same complex (Scheme 1). The structure we now propose for 1 is supported by the recently determined X-ray structures of the derivatives $[Ru_3(\mu\text{-H})(\mu_3\text{-ampy})(\mu\text{-}\eta^1\text{:}\eta^2\text{-PhC=CHPh})(CO)_8][BF_4]$ (this work), $[Ru_3(\mu_3\text{-ampy})(\mu\text{-}\eta^1\text{:}\eta^2\text{-PhC=CHPh})(CO)_7(PCy_3)]$,^{12c} and $[Ru_3(\mu_3\text{-ampy})(\mu\text{-}\eta^1\text{:}\eta^2\text{-PhC=CHPh})(CO)_6(PPh_3)_2]$.^{12d} Most probably, the phenyl group of the anilino-6-methylpyridinato fragment of $[Ru_3(\mu_3\text{-ampy})(\mu\text{-}\eta^1\text{:}\eta^2\text{-PhC=CHPh})(CO)_8]$ forces the alkenyl ligand to bridge a different Ru–Ru edge. (a) Cabeza, J. A.; García-Granda, S.; Llamazares, A.; Riera, V.; Van der Maelen, J. F. *Organometallics* **1993**, *12*, 157. (b) Cabeza, J. A.; García-Granda, S.; Llamazares, A.; Riera, V.; Van der Maelen, J. F. *Organometallics* **1993**, *12*, 2973. (c) Cabeza, J. A.; Ouahab, L. Unpublished results. (d) Cabeza, J. A.; Llamazares, A.; Riera, V.; Briard, P.; Ouahab, L. *J. Organomet. Chem.*, in press.

(13) Andreu, P. L.; Cabeza, J. A.; Riera, V.; Jeannin, Y.; Miguel, D. *J. Chem. Soc., Dalton Trans.* **1990**, 2201.

Table 1. Kinetic Data for the Hydrogenation of Diphenylacetylene Promoted by Complex 1 in Toluene at 333 K

$P(\text{H}_2)/\text{atm}$	$10^3[\text{I}]/\text{M}$	$[\text{Ph}_2\text{C}_2]/\text{M}$	$10^6(-dV/dt)/(\text{L s}^{-1})$
0.364	8.45	0.070	8.70
0.491	8.45	0.070	10.30
0.685	8.45	0.070	14.21
0.838	8.45	0.070	17.30
0.359	3.07	0.205	2.18
0.501	3.07	0.205	2.85
0.633	3.07	0.205	3.55
0.838	3.07	0.205	5.26
0.838	0.77	0.070	2.27
0.838	1.54	0.070	4.15
0.838	3.07	0.070	8.53
0.838	4.60	0.070	12.10
0.838	8.45	0.070	17.30
0.838	0.77	0.205	1.31
0.838	1.54	0.205	2.06
0.838	4.60	0.205	6.25
0.838	3.07	0.035	12.52
0.838	3.07	0.140	5.72
0.838	3.07	0.315	4.63
0.838	3.07	0.421	4.75

absence of complex 1 and the presence of the known compounds **2**¹³ and **3**.¹¹ The solution was evaporated to dryness and the residue analyzed by ¹H NMR spectroscopy, which indicated a ca. 2:1 mol ratio for compounds **2** and **3**.

Preparation of [Ru₃(μ₃-ampy)(η¹-PhC=CHPh)(CO)₉] (4). Carbon monoxide was bubbled through a THF (15 mL) solution of complex 1 (33 mg, 0.040 mmol) for 10 min. The color changed from deep red to orange. The IR spectrum of a CO-saturated solution showed the complete disappearance of compound 1 and the formation of a new product (4). IR (ν(CO); THF): 2074 (w), 2047 (s), 2014 (s), 1974 (s, br), 1942 (w) cm⁻¹. This compound was not isolated as a solid because the reaction proved to be reversible: complex 1 was readily re-formed when a nitrogen atmosphere was substituted for the CO atmosphere. However, the compound could also be characterized by NMR spectroscopy; the reaction was carried out in a deuterated solvent, and the NMR tube was sealed under a CO atmosphere. ¹H NMR (benzene-*d*₆, 23 °C): 7.64 (s, 1 H, alkenyl =CH), 7.34 (m, 2 H), 7.14 (m, 4 H), 6.88 (m, 4 H), 6.35 (t, *J* = 7.6 Hz, 1 H, ampy H⁴), 5.80 (d, *J* = 7.6 Hz, 1 H, ampy H⁵), 5.03 (d, br, *J* = 7.6 Hz, 1 H, ampy H³), 3.69 (s, br, 1 H, ampy NH), 2.11 (s, 3 H, ampy Me) ppm. Selected ¹³C{¹H} NMR (toluene-*d*₈, -70 °C): 206.2, 204.7, 204.3, 203.4, 202.6, 201.9, 201.6, 189.1, 181.5 (9 CO ligands) ppm; 180.1, 160.6, 137.9, 120.4, 105.7, 29.5 (ampy carbon atoms) ppm; 155.9 (alkenyl C=CH) ppm; 140.4 (alkenyl C=CH) ppm.

Preparation of [Ru₃(μ-H)(μ₃-ampy)(μ-η¹:η²-PhC=CHPh)(CO)₉][BF₄] (5). An excess of HBF₄·OEt₂ (ca. 0.2 mL) was added to a dichloromethane solution (10 mL) of complex 1 (162 mg, 0.199 mmol). The color changed from deep red to orange. The solvent was removed under reduced pressure and the oily residue washed with diethyl ether (3 × 10 mL) to give complex 5 as a red-orange powder (160 mg, 89%). Anal. Calcd for C₂₈H₁₉BF₄N₂O₈Ru₃: C, 37.31; H, 2.12; N, 3.12. Found: C, 37.19; H, 1.98; N, 3.03. IR (ν(CO); CH₂Cl₂): 2109 (m), 2088 (s), 2055 (s), 2035 (s), 2000 (m) cm⁻¹. ¹H NMR (acetone-*d*₆, 23 °C): 7.89 (t, *J* = 7.7 Hz, 1 H), 7.6–6.5 (complex mixture of signals), 6.25 (s, br, 1 H, ampy NH), 5.46 (s, 1 H, alkenyl =CH), 3.04 (s, 3 H, ampy Me), -11.77 (s, 1 H, μ-H) ppm. Selected ¹³C{¹H} NMR data (dichloromethane-*d*₂, 23 °C): 198.0, 197.9, 194.3, 192.8, 192.0, 190.0, 188.2, 182.3 (8 CO ligands) ppm; 176.7, 152.6, 141.9, 122.4, 115.2, 30.8 (ampy carbon atoms) ppm; 219.4 (alkenyl C=CH) ppm; 80.3 (alkenyl C=CH) ppm.

Reaction of Complex 5 with [PPN][BH₄]. The addition of [PPN][BH₄] (16.5 mg, 0.030 mmol) to a dichloromethane solution (6 mL) of complex 5 (26.5 mg, 0.029 mmol) caused an immediate color change from orange to red and the complete disappearance of complex 5 (IR). A GC analysis of the solution showed *cis*- and *trans*-stilbene as the only organic products.

Table 2. Crystallographic and Refinement Data for 5-CH₂Cl₂

formula	C ₂₈ H ₁₉ BF ₄ N ₂ O ₈ Ru ₃ ·CH ₂ Cl ₂
fw	986.40
cryst syst	triclinic
space group	P $\bar{1}$
<i>a</i> , <i>b</i> , <i>c</i> , Å	10.357(9), 11.279(5), 16.751(9)
α , β , γ , deg	105.42(6), 97.68(6), 100.61(4)
<i>V</i> , Å ³	1819(2)
<i>Z</i>	2
<i>F</i> (000)	960
<i>D</i> _{calcd} , g/cm ³	1.80
μ , cm ⁻¹	14.20
min, max cor factors	0.99, 1.07
cryst size, mm	0.13 × 0.10 × 0.10
radiation (λ , Å)	Mo K α (0.710 73)
diffractometer	Enraf-Nonius CAD4
monochromator	graphite
temp, K	293(2)
scan method	ω -2 θ
<i>hkl</i> range	±12; ±13; 0–19
θ range, deg	1.29–24.98
no. of measd rflns	6645
no. of unique rflns	6405
<i>R</i> _{int} = $\sum(I - \langle I \rangle)/\sum I$	0.052
no. of rflns with <i>I</i> > 2 σ (<i>I</i>)	2638
no. of variables	481
<i>R</i> (<i>F</i>) _{<i>I</i>>2σ(<i>I</i>)} ^a	0.0695
<i>R</i> _w (<i>F</i> ²) _{all data} ^b	0.1842
GOF ^c	0.881
$\Delta\rho$	0.04
max, min $\Delta\rho$, e/Å ³	1.273, -1.559 ^d

^a $R(F) = \sum||F_o| - |F_c||/\sum|F_o|$. ^b $R_w(F^2) = [\sum w(F_o^2 - F_c^2)^2/\sum w(F_o^2)^2]^{1/2}$. ^c Goodness of fit (GOF) = $[\sum w(F_o^2 - F_c^2)^2/(N - P)]^{1/2}$. ^d Close to the disordered CH₂Cl₂ molecule.

The solution was evaporated to dryness and the residue analyzed by qualitative TLC and ¹H NMR spectroscopy; both showed the presence of a complex mixture of unidentified products.

Reaction of Complex 5 with [PPN][BH₄] in the Presence of Diphenylacetylene. [PPN][BH₄] (33.7 mg, 0.063 mmol) was added to a solution of complex 5 (57 mg, 0.063 mmol) and diphenylacetylene (11.5 mg, 0.063 mmol) in dichloromethane (10 mL). The solution immediately changed from orange to deep red, while its IR spectrum indicated the complete transformation of complex 5 into complex 1. *cis*- and *trans*-stilbene were also observed in a GC analysis of the solution.

Crystal Structure of 5-CH₂Cl₂. A red crystal of 5-CH₂Cl₂, obtained by layering pentane on a solution of the complex in dichloromethane, was used for the X-ray diffraction study. A selection of crystal and refinement data is given in Table 2.

The cell dimensions were determined by least-squares refinement of 25 reflections with 15 < θ < 17°. The intensities were collected using the ω -2 θ scan technique with a variable scan rate and a maximum scan time of 60 s per reflection. Three standard reflections were monitored every 60 min, revealing no intensity fluctuations. Profile analysis was performed on all reflections.¹⁴ Lorentz and polarization effects were corrected and the data were reduced to $|F_o|$ values.

The structure was solved by Patterson interpretation using DIRDIF92.¹⁵ Isotropic least-squares refinement, using a local version¹⁶ of SHELX,¹⁷ was followed by a semiempirical absorption correction¹⁸ (maximum and minimum correction factors

(14) (a) Lehman, M. S.; Larsen, F. K. *Acta Crystallogr.* **1974**, *A30*, 580. (b) Grant, D. F.; Gabe, E. J. *J. Appl. Crystallogr.* **1978**, *11*, 114.

(15) Beurskens, P. T.; Admiraal, G.; Beurskens, G.; Bosman, W. P.; Garcia-Granda, S.; Gould, R. O.; Smits, J. M. M.; Smykalla, C. The DIRDIF92 Program System, University of Nijmegen: Nijmegen, The Netherlands, 1992.

(16) Van der Maelen, J. F. Ph.D. Thesis, University of Oviedo, Oviedo, Spain, 1991.

(17) Sheldrick, G. M. SHELX, a Program for Crystal Structure Determination; University Chemical Laboratory: Cambridge, U.K., 1976.

1.21 and 0.44, respectively). Full-matrix anisotropic least-squares refinement over F^2 , using the program SHELXL93,¹⁹ followed by a difference Fourier synthesis allowed the location of all the hydrogen atoms. After refinement of the positional and anisotropic thermal parameters of the non-hydrogen atoms, the hydrogen atoms were refined isotropically using a riding model (with one common thermal parameter for the hydrogens of the methyl group and other for the remaining hydrogen atoms) except for H(1) and H(2) (whose distances to Ru(2) and Ru(3), and N(1), respectively, were restrained to chemically acceptable values) and H(16) (which was left free). A dichloromethane solvent molecule, disordered in two positions with occupation factors of 0.70(2) and 0.30(2), was refined restraining all equivalent distances and all displacement parameters along the bond directions. The function minimized was $\sum w(F_o^2 - F_c^2)^2$; $w = 1/[\sigma^2(F_o^2) + (0.0996P)^2]$, with $\sigma(F_o)$ obtained from counting statistics and $P = (F_o^2 + 2F_c^2)/3$. Atomic scattering factors were taken from ref 20. Geometrical calculations were made with PARST.²¹ The structure plot was drawn with the EUCLID package.²² Positional parameters for the non-hydrogen atoms of $5\text{-CH}_2\text{Cl}_2$ are given in Table 3.

Results

Catalytic Hydrogenation of Diphenylacetylene Promoted by 1. Complex 1 has been found to be a catalyst precursor for the homogeneous hydrogenation of diphenylacetylene under mild conditions (turnover frequency 38.8 h^{-1} , in toluene at 333 K for $[1] = 3.07 \times 10^{-3} \text{ M}$, $[\text{Ph}_2\text{C}_2] = 0.205 \text{ M}$, and $P(\text{H}_2) = 0.838 \text{ atm}$), rendering a mixture of *cis*- and *trans*-stilbene (Figure 1); *cis*-stilbene is the kinetic product, since the *cis*- to *trans*-stilbene ratio decreases continuously as the hydrogenation of the alkyne progresses. Hydrogenation of stilbene to 1,2-diphenylethane was not detected, even at high conversions. It is important to note that compound 1 was the only metal complex observed in the catalytic solutions by IR spectroscopy, at high and low [substrate]:[catalyst] ratios. No hydrogenation was observed at room temperature except when very low [substrate]:[catalyst] ratios were used (turnover frequency ca. 3.2 h^{-1} at $[\text{Ph}_2\text{C}_2]:[1] = 6$).

Hydrogenation rates ($-dV/dt$) were obtained at 333 K by measuring the hydrogen uptake as a function of time, with correction for the volume of consumed hydrogen to that corresponding to 1 atm (V_c), as shown in Figure 2. We used data corresponding to the first 8 min of reaction in order to base the kinetic analysis on initial rates.

In order to determine the rate dependence on each reagent, runs were carried out with the concentration of the other two reagents kept constant (Table 1). The dependence of the rate of hydrogen consumption on substrate concentration (Figure 3) was found to be not linear: at high $[\text{Ph}_2\text{C}_2]:[1]$ ratios the rate does not depend on substrate concentration, whereas at low $[\text{Ph}_2\text{C}_2]:[1]$ ratios the rate decreases as the concentration of substrate increases. At a moderately high diphenylacetylene concentration (0.205 M), plots of $\log(-dV/dt)$ vs $\log P(\text{H}_2)$ and $\log(-dV/dt)$ vs $\log [1]$ afforded straight lines of slopes 1.04 and 0.95, respectively (Figure 4),

Table 3. Fractional Atomic Coordinates ($\times 10^4$) and Isotropic Temperature Factors ($\times 10^3$) for $5\text{-CH}_2\text{Cl}_2$

atom	<i>x/a</i>	<i>y/b</i>	<i>z/c</i>	$U_{eq}, \text{\AA}^2$
Ru(1)	155(1)	2652(1)	1482(1)	36(1)
Ru(2)	-535(1)	3148(1)	2995(1)	35(1)
Ru(3)	-1322(1)	4548(1)	1925(1)	39(1)
C(1)	1651(15)	3785(14)	1355(10)	57(4)
O(1)	2554(12)	4482(10)	1299(8)	83(4)
C(2)	-805(16)	2558(14)	390(11)	59(4)
O(2)	-1388(13)	2406(10)	-272(8)	78(4)
C(3)	845(15)	1197(13)	1006(9)	52(4)
O(3)	1358(11)	385(10)	791(7)	77(3)
C(4)	-1527(14)	2513(14)	3743(10)	55(4)
O(4)	-2117(12)	2083(11)	4153(8)	83(4)
C(5)	444(16)	4417(16)	3877(12)	64(5)
O(5)	1057(13)	5319(12)	4492(8)	88(4)
C(6)	-1217(14)	5051(12)	917(9)	46(4)
O(6)	-1108(12)	5373(10)	345(7)	74(3)
C(7)	291(17)	5756(13)	2499(11)	59(4)
O(7)	1208(12)	6539(11)	2824(8)	85(4)
C(8)	-2368(15)	5733(13)	2373(10)	54(4)
O(8)	-2894(12)	6446(11)	2678(8)	85(4)
N(1)	-1574(10)	1838(9)	1860(7)	40(3)
N(2)	-3020(10)	2946(9)	1344(7)	41(3)
C(9)	-2874(12)	1831(11)	1493(7)	33(3)
C(10)	-3930(14)	794(11)	1289(9)	47(4)
C(11)	-5156(15)	860(13)	927(10)	57(4)
C(12)	-5318(14)	1970(13)	728(10)	53(4)
C(13)	-4240(15)	2968(14)	936(9)	56(4)
C(14)	-4401(16)	4153(14)	721(10)	68(5)
C(15)	1190(12)	2478(11)	2596(8)	41(3)
C(16)	539(13)	1565(11)	2968(9)	44(4)
C(17)	2642(13)	3098(13)	2941(10)	51(4)
C(18)	3524(15)	2308(15)	2952(11)	67(5)
C(19)	4894(16)	2774(20)	3212(13)	90(6)
C(20)	5397(18)	4083(23)	3496(13)	103(7)
C(21)	4529(17)	4892(17)	3499(14)	94(7)
C(22)	3187(14)	4392(15)	3218(10)	63(4)
C(23)	1127(13)	1305(14)	3780(10)	50(4)
C(24)	1882(16)	2198(15)	4475(11)	70(5)
C(25)	2373(18)	1908(21)	5204(12)	94(6)
C(26)	2056(25)	634(27)	5143(16)	139(11)
C(27)	1346(23)	-259(21)	4442(16)	132(11)
C(28)	852(17)	62(16)	3758(11)	76(5)
B(1)	1786(23)	1786(16)	8631(13)	72(6)
F(1)	713(10)	2181(9)	8282(7)	96(3)
F(2)	2830(11)	2771(9)	8982(7)	102(4)
F(3)	2087(10)	879(9)	7990(7)	98(4)
F(4)	1428(13)	1175(13)	9209(10)	155(6)
C(29)	4156(210)	9279(156)	3899(88)	327(28)
Cl(1)	4652(71)	9408(58)	3098(47)	314(20)
Cl(2)	4198(54)	8420(44)	4473(40)	321(22)
C(29')	4815(53)	8133(43)	2464(21)	277(17)
Cl(1')	3790(21)	8000(22)	1702(15)	376(16)
Cl(2')	4519(32)	8527(36)	3351(24)	375(15)

^a U_{eq} is equal to one-third of the trace of the orthogonalized U_{ij} tensor.

indicating that the hydrogenation reaction is first order in hydrogen pressure and first order in the concentration of added 1 at high $[\text{Ph}_2\text{C}_2]:[1]$ ratios. Similar plots for data taken at $[\text{Ph}_2\text{C}_2] = 0.070 \text{ M}$ gave slopes of 0.84 and 0.95, respectively, indicating that at low $[\text{Ph}_2\text{C}_2]:[1]$ ratios the hydrogenation reaction is also first order in hydrogen pressure and in the concentration of added 1.

Considering the possibility of carbon monoxide dissociation from complex 1 during the catalysis, we studied the effect that the addition of small amounts of this gas into the reacting solutions produced on the hydrogenation rate: a strong reduction of the rate was observed (Figure 5). However, this result does not necessarily imply the existence of a CO dissociation step in the catalytic mechanism, because CO is an excellent ligand which may compete with other reagents for the vacant coordination sites available in the reaction

(18) Walker, N.; Stuart, D. *Acta Crystallogr.* **1983**, A39, 158.

(19) Sheldrick, G. M. *J. Appl. Crystallogr.*, in press.

(20) *International Tables for X-Ray Crystallography*; Kynoch Press: Birmingham, U.K., 1974 (present distributor Kluwer: Dordrecht, The Netherlands); Vol. 4.

(21) Nardelli, M. *Comput. Chem.* **1983**, 7, 95.

(22) Spek, A. L. In *Computational Crystallography*; Sayre, D., Ed.; Clarendon Press: Oxford, U.K., 1982; p 528.

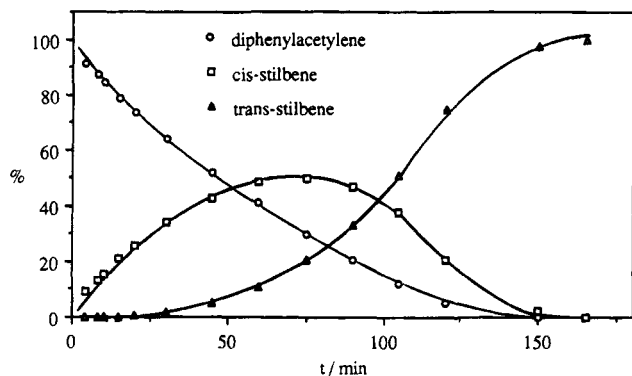


Figure 1. Evolution of the catalytic hydrogenation of diphenylacetylene promoted by complex **1** (toluene, 333 K, $[1] = 3.07 \times 10^{-3}$ M, $[\text{Ph}_2\text{C}_2] = 0.205$ M, $P(\text{H}_2) = 0.838$ atm).

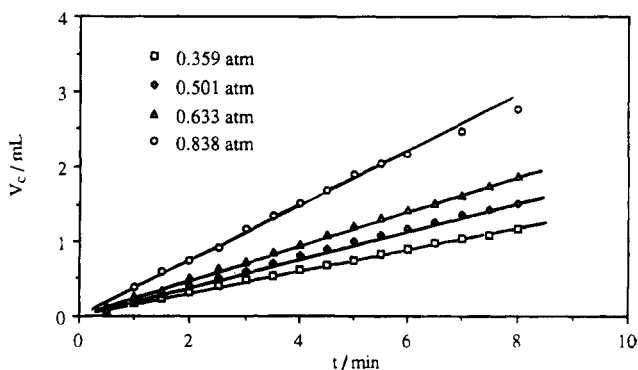


Figure 2. Hydrogen-uptake plots, at different hydrogen pressures, for the hydrogenation of diphenylacetylene promoted by **1** (toluene, 333 K, $[1] = 3.07 \times 10^{-3}$ M, $[\text{Ph}_2\text{C}_2] = 0.205$ M).

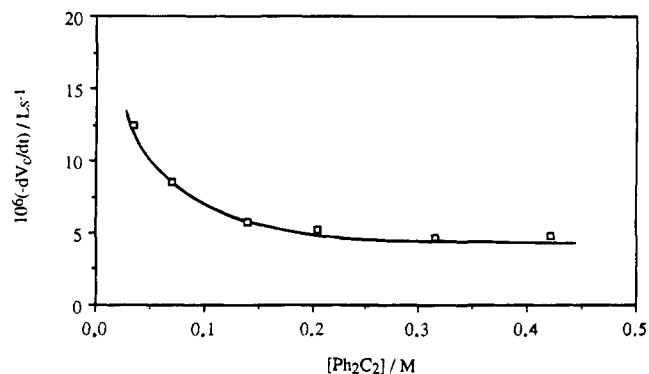


Figure 3. Plot of the reaction rate dependence on substrate concentration for the hydrogenation of diphenylacetylene promoted by **1** (toluene, 333 K, $[1] = 3.07 \times 10^{-3}$ M, $P(\text{H}_2) = 0.838$ atm).

intermediates. Unfortunately, a rigorous kinetic study of the CO dependence of the hydrogenation reaction could not be carried out with our experimental equipment.

Reactions of Cluster 1 Relevant to the Catalytic Hydrogenation Process. In order to gain further knowledge about the molecular aspects of the catalytic process, some reactions of the catalytic precursor **1** were studied.

At room temperature, complex **1** reacted with hydrogen (1 atm), in the absence of diphenylacetylene, to give a mixture of *cis*- and *trans*-stilbene and the known cluster compounds $[\text{Ru}_3(\mu\text{-H})(\mu_3\text{-ampy})(\text{CO})_9]^{13}$ (**2**) and $[\text{Ru}_6(\mu\text{-H})_6(\mu_3\text{-ampy})_2(\text{CO})_{14}]^{11}$ (**3**) (Scheme 1); however,

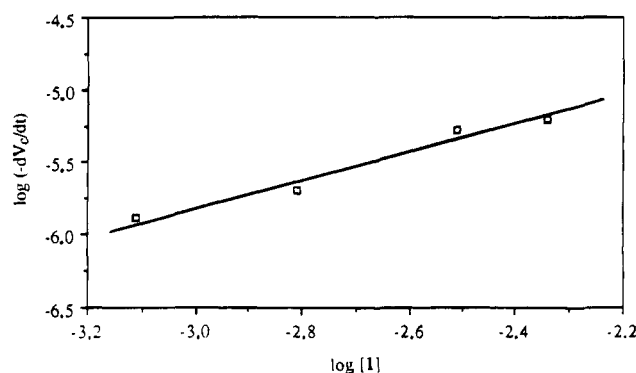
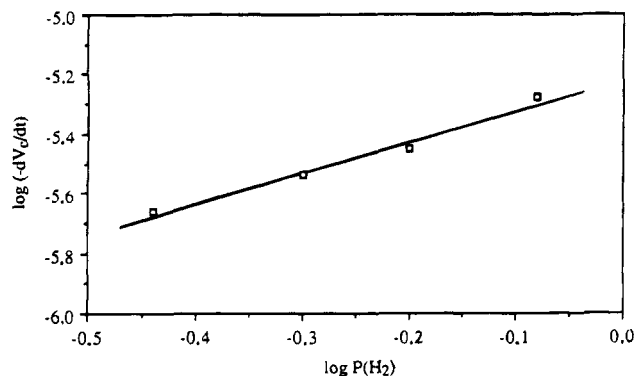


Figure 4. Partial reaction orders with respect to $P(\text{H}_2)$ (top) and $[1]$ (bottom) for the hydrogenation of diphenylacetylene promoted by **1** when $[\text{Ph}_2\text{C}_2] = 0.205$ M (toluene, 333 K).

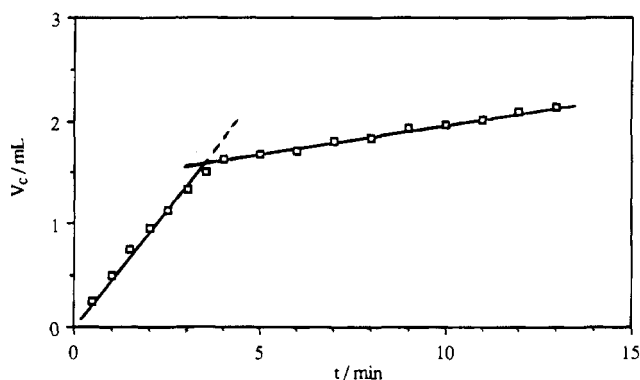


Figure 5. Effect of the addition of carbon monoxide (5 mL, at $t = 3.5$ min) on the hydrogenation rate (toluene, 333 K, $[1] = 3.07 \times 10^{-3}$ M, $P(\text{H}_2) = 0.838$ atm, $[\text{Ph}_2\text{C}_2] = 0.205$ M).

although a very slow catalytic hydrogenation reaction was observed at low [substrate]:[catalyst] ratios (<10), no reaction was observed when more diphenylacetylene was present in solution. These results suggest that in the catalytic hydrogenation reaction, for low [substrate]:[catalyst] ratios, complex **1** releases diphenylacetylene prior to its reaction with hydrogen to give an unsaturated species (at room temperature, when the solution contains diphenylacetylene, this equilibrium seems to be completely displaced to the left), which is responsible for the hydrogenation of diphenylacetylene and for the subsequent formation of complexes **2** and **3** (as final decomposition products) when all the substrate has been consumed.

Complex **1** reacted with carbon monoxide, under very mild conditions (10 min, 20 °C, 1 atm), to give the nonacarbonyl derivative $[\text{Ru}_3(\mu_3\text{-ampy})(\eta^1\text{-PhC}=\text{CHPh})$

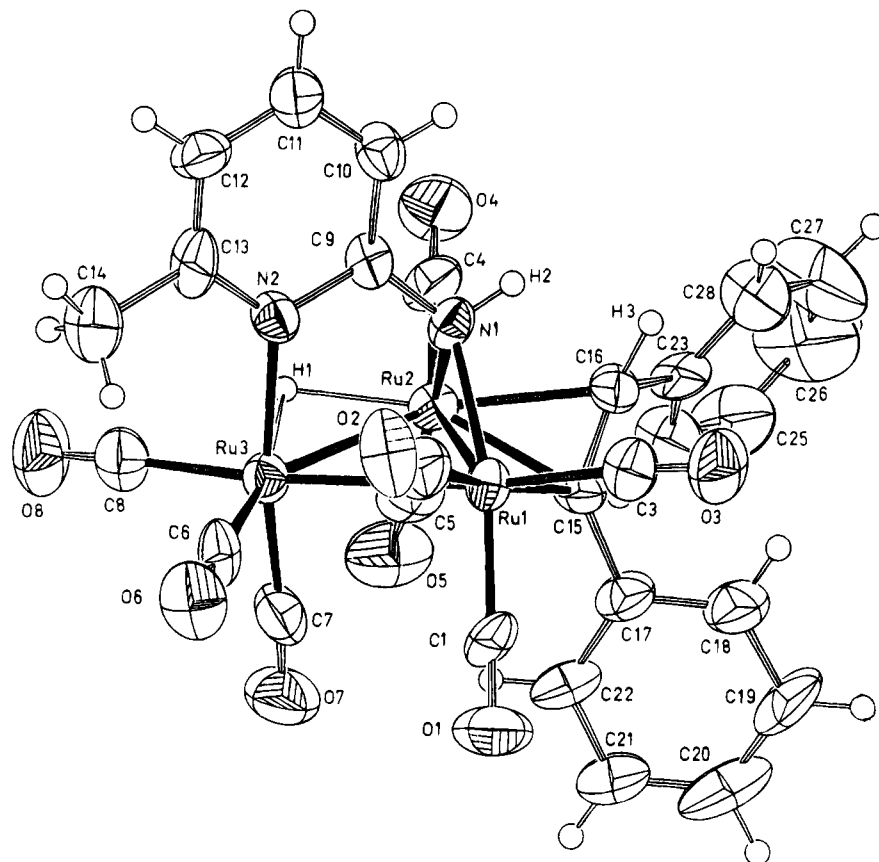


Figure 6. EUCLID plot of the cation $[\text{Ru}_3(\mu\text{-H})(\mu_3\text{-ampy})(\mu\text{-}\eta^1:\eta^2\text{-PhC=CHPh})(\text{CO})_8]^+$ in $5\text{-CH}_2\text{Cl}_2$.

(CO)₉ (4). This compound, which is the first characterized example of a cluster complex containing a terminal alkenyl ligand, is stable only under a carbon monoxide atmosphere, reverting to complex 1 under nitrogen or under vacuum. The structure proposed for complex 4 in Scheme 1 is based on its IR (which only shows terminal CO ligands) and NMR spectroscopic data. The number of CO ligands was easily deduced from the ¹³C-¹H NMR spectrum (run at -70 °C because the compound shows CO fluxionality at room temperature), which contains nine singlets in the CO region. The ¹H and ¹³C NMR absorptions of the alkenyl =CH fragment appear at 7.64 and 140.4 ppm, respectively, confirming that the alkenyl group is not $\mu\text{-}\eta^1:\eta^2$ -coordinated, because otherwise the resonances of its =CH moiety would appear at lower chemical shifts.²³ This transformation of the alkenyl ligand of 1 from bridging to terminal may well have mechanistic implications in the catalytic hydrogenation of diphenylacetylene promoted by complex 1.

The sequential addition of a proton and a hydride to a metal complex may, in some instances, be considered equivalent to the oxidative addition of a hydrogen molecule. Having this in mind, we carried out the sequential reactions of complex 1 with protons and hydrides.

Complex 1 reacted with HBF₄·OEt₂ to give the cationic hydrido derivative $[\text{Ru}_3(\mu\text{-H})(\mu_3\text{-ampy})(\mu\text{-}\eta^1:\eta^2\text{-PhC=CHPh})(\text{CO})_8][\text{BF}_4]$ (5) quantitatively. Its ¹H and ¹³C{¹H} NMR spectra confirmed the presence of hydrido, alkenyl, and ampy ligands but were insufficient

Table 4. Selected Bond Lengths and Bond Angles in $5\text{-CH}_2\text{Cl}_2$

Bond Lengths (Å)			
Ru(1)–Ru(2)	2.669(2)	Ru(1)–Ru(3)	2.850(2)
Ru(2)–Ru(3)	2.822(2)	Ru(1)–N(1)	2.11(1)
Ru(2)–N(1)	2.08(1)	Ru(3)–N(2)	2.18(1)
Ru(1)–C(1)	1.89(2)	Ru(1)–C(2)	1.93(2)
Ru(1)–C(3)	1.93(1)	Ru(2)–C(4)	1.92(2)
Ru(2)–C(5)	1.79(2)	Ru(3)–C(6)	1.93(1)
Ru(3)–C(7)	1.90(2)	Ru(3)–C(8)	1.93(1)
Ru(1)–C(15)	2.10(1)	Ru(2)–C(15)	2.18(1)
Ru(2)–C(16)	2.26(1)	C(15)–C(16)	1.45(2)
Ru(2)–H(1)	1.9(1)	Ru(3)–H(1)	2.0(1)
Bond Angles (deg)			
Ru(1)–Ru(2)–Ru(3)	62.47(5)	Ru(1)–Ru(3)–Ru(2)	56.14(5)
Ru(2)–Ru(1)–Ru(3)	61.39(6)	C(15)–Ru(1)–Ru(2)	52.8(4)
C(15)–Ru(1)–Ru(3)	108.5(4)	C(15)–Ru(2)–Ru(1)	50.1(3)
C(15)–Ru(2)–Ru(3)	107.1(3)	C(16)–Ru(2)–Ru(1)	76.3(4)
C(16)–Ru(2)–Ru(3)	138.4(4)	C(15)–Ru(2)–C(16)	38.0(4)
Ru(1)–C(15)–Ru(2)	77.1(4)	C(16)–C(15)–Ru(1)	118.3(9)
C(16)–C(15)–Ru(2)	74.2(7)	C(15)–C(16)–Ru(2)	67.9(7)

to unambiguously assign a structure; therefore, a single-crystal X-ray diffraction study (of the solvate $5\text{-CH}_2\text{Cl}_2$) was carried out (Figure 6, Table 4). The most interesting features of this structure are that the alkenyl ligand spans the same Ru–Ru edge as the amido fragment of the ampy ligand and that the hydrido ligand is approximately trans to the coordinated double bond of the alkenyl moiety.

The addition of [PPN][BH₄] to a dichloromethane solution of complex 5 (1:1 equivalent ratio, room temperature) caused the immediate disappearance of complex 5. A GC analysis of the solution showed *cis*- and *trans*-stilbene as the only organic products. The solution was evaporated to dryness and the residue analyzed by qualitative TLC and ¹H NMR spectroscopy, showing

(23) The ¹H and ¹³C NMR resonances of the alkenyl =CH moiety of complex 1 appear at 4.09 and 80.5 ppm, respectively.¹⁰

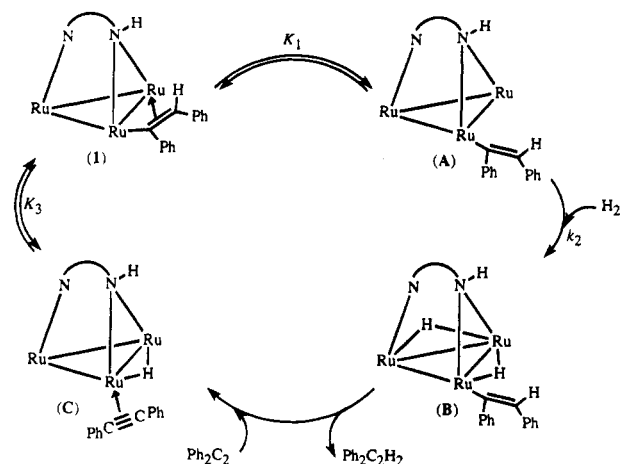


Figure 7. Proposed mechanism for the hydrogenation of diphenylacetylene promoted by complex **1**, at high $[\text{Ph}_2\text{C}_2]:[\mathbf{1}]$ ratios. Carbonyl ligands have been omitted for clarity.

the presence of a complicated mixture of complexes. All attempts to characterize any dihydrido intermediates by NMR spectroscopy, with the reaction being carried out in an NMR tube at low temperature (-60 to 0 °C), were unsuccessful. Interestingly, when the room-temperature reaction of complex **5** with $[\text{PPN}][\text{BH}_4]$ was carried out in the presence of diphenylacetylene, *cis*- and *trans*-stilbene were also formed, but compound **1** was the only metal complex observed in the solution.

Discussion

Mechanistic Aspects of the Homogeneous Hydrogenation of Diphenylacetylene Promoted by Complex 1. The observed reaction rate dependence on substrate concentration (Figure 3) suggests that the mechanism consists of two different catalytic cycles, each operating at different $[\text{substrate}]:[\text{catalyst}]$ ratios.

A reaction pathway for the homogeneous hydrogenation of diphenylacetylene promoted by complex **1**, at high $[\text{Ph}_2\text{C}_2]:[\mathbf{1}]$ ratios, is proposed in Figure 7. It involves the decoordination of the alkenyl C=C moiety of **1** to give the intermediate **A** (K_1), a coordinatively unsaturated η^1 -alkenyl species, which subsequently reacts with hydrogen to give **B** (k_2). A fast hydride transfer to the alkenyl ligand (both ligands are in the appropriate *cis* arrangement)⁵ produces *cis*-stilbene, which is rapidly replaced by a new molecule of alkyne to close the catalytic cycle.

We have previously reported that, in the hydrogenation of diphenylacetylene promoted by $[\text{Ru}_3(\mu_3\text{-ampy})(\mu\text{-}\eta^1\text{-}\eta^2\text{-PhC=CHPh})(\text{CO})_7(\text{PPh}_3)]$, the cluster undergoes activation through a CO dissociation step.⁵ However, in the present case, the mild conditions required for the synthesis of the η^1 -alkenyl derivative **4** from complex **1** indicate that the transformation of the alkenyl group in **1** from bridging to terminal is a low-energy process, and the fact that complex **4** was never observed in the catalytic solutions suggests the absence of a CO dissociation step in the hydrogenation mechanism. Moreover, the facile formation of complex **4** from **1** and carbon monoxide may also explain why the rate of hydrogenation of diphenylacetylene decreased when CO was added into the system (Figure 5). Although the existence of a CO dissociation step will fit the available kinetic data equally well, such a step is not supported by the results

of the stoichiometric reactions described above (see also the next paragraph).

As noted above, the sequential addition of a proton and a hydride to a metal complex may be considered equivalent to the oxidative addition of dihydrogen, and we have shown that complex **1** was re-formed when it was sequentially treated with HBF_4 (to give **5**) and then with $[\text{PPN}][\text{BH}_4]$ in the presence of diphenylacetylene (*cis*- and *trans*-stilbene were also produced in this reaction). However, a vacant coordination site in **5** is needed prior to its reaction with $[\text{PPN}][\text{BH}_4]$. The fact that **1** and **5** contain the same number of carbonyl ligands supports the hypothesis that the vacant sites needed for the reactions of **1** with hydrogen (at high $[\text{Ph}_2\text{C}_2]:[\mathbf{1}]$ ratios) and of **5** with $[\text{BH}_4]^-$ arise from a bridging to terminal transformation of the alkenyl groups in **1** and **5** instead of from a CO dissociation process.

If the addition of hydrogen to **A** is the rate-determining step (k_2), this cycle (Figure 7) is also compatible with the fact that compound **1** is the only complex spectroscopically observed during the catalysis, because K_1 should have a very small value (in fact, **A** has never been detected in solutions of complex **1**). Furthermore, the results obtained from the room-temperature reaction of the cationic complex **5** with $[\text{PPN}][\text{BH}_4]$ also confirm that k_2 is the slowest step in the catalytic cycle. In this stoichiometric reaction, a neutral dihydrido species, which is probably **B**, should be formed; this elusive species rapidly releases *cis*-stilbene at room temperature to give an unsaturated derivative which then reacts with diphenylacetylene to give **1** (or decomposes if no alkyne is available). Therefore, as no catalytic hydrogenation was observed at room temperature at high $[\text{substrate}]:[\text{catalyst}]$ ratios, the rate-determining step of the catalytic cycle should be prior to the elimination of stilbene from **B**.

According to the proposed mechanism (Figure 7), since the volume of consumed hydrogen is directly related to the disappearance of diphenylacetylene, the rate law may be given as

$$v_1 = -d[\text{Ph}_2\text{C}_2]/dt = k_2[\mathbf{A}](P(\text{H}_2))$$

But $[\mathbf{A}]$ can be expressed as a function of $[\mathbf{1}]$ through the equilibrium constant K_1 ; thus

$$v_1 = -d[\text{Ph}_2\text{C}_2]/dt = K_1 k_2 [\mathbf{1}](P(\text{H}_2))$$

This rate law, which is zero order in diphenylacetylene concentration, agrees well with our experimental kinetic data obtained at high $[\text{Ph}_2\text{C}_2]:[\mathbf{1}]$ ratios.

On the other hand, Figure 8 proposes a reaction pathway for the homogeneous hydrogenation of diphenylacetylene promoted by complex **1**, at low $[\text{Ph}_2\text{C}_2]:[\mathbf{1}]$ ratios. The actual catalytic cycle is preceded by two equilibria which transform complex **1** into the hydrido-alkyne intermediate **C** (K_3) and then, via decoordination of diphenylacetylene (K_4), into the unsaturated species **D**; addition of hydrogen to **D** (k_5) leads to a trihydrido intermediate (**E**) which after a fast reaction with diphenylacetylene releases stilbene, regenerating **D**.

The results obtained from the reaction of complex **1** with hydrogen, with and without diphenylacetylene in the solution, and the negative rate dependence in substrate concentration experimentally obtained for the

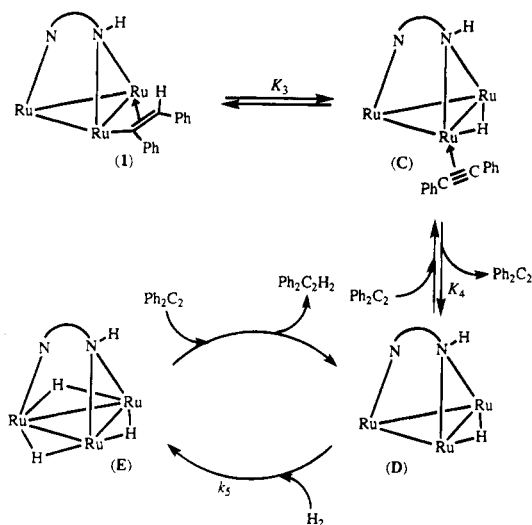


Figure 8. Proposed mechanism for the hydrogenation of diphenylacetylene promoted by complex **1**, at low $[\text{Ph}_2\text{C}_2]:[\mathbf{1}]$ ratios. Carbonyl ligands have been omitted for clarity.

catalytic hydrogenation at low $[\text{Ph}_2\text{C}_2]:[\mathbf{1}]$ ratios, confirm that, under these conditions, complex **1** dissociates diphenylacetylene prior to the rate-determining step, which is likely to be the oxidative addition of hydrogen (k_5) because the reaction is first order in hydrogen pressure. However, the nature of the fast steps that lead from **E** to **D** remains unknown.

This mechanism (Figure 8) is also compatible with the fact that compound **1** is the only complex observed during the catalysis, because the equilibria defined by K_3 and K_4 should be largely displaced to the left (**C** and **D** have never been observed in solutions of complex **1**).

Consequently, the hydrogenation rate may be given as

$$v_2 = -d[\text{Ph}_2\text{C}_2]/dt = k_5[\mathbf{D}](P(\text{H}_2))$$

However, $[\mathbf{D}]$ can be expressed as a function of $[\mathbf{1}]$ through the equilibrium constants K_4 and K_3 ; thus

$$v_2 = -d[\text{Ph}_2\text{C}_2]/dt = K_3K_4k_5[\mathbf{1}](P(\text{H}_2))[\text{Ph}_2\text{C}_2]^{-1}$$

This rate law, which is negative order in substrate concentration, agrees well with our experimental kinetic data obtained at low $[\text{Ph}_2\text{C}_2]:[\mathbf{1}]$ ratios.

However, in a general case, the catalytic cycles shown in Figures 7 and 8 should not be separated because both should contribute to the hydrogenation reaction (in fact they have common intermediates), with individual contributions depending on the particular $[\text{Ph}_2\text{C}_2]:[\mathbf{1}]$ ratio. Thus, from Figure 3 it can be deduced that the cycle shown in Figure 7 is more operative than that shown in Figure 8 at $[\text{Ph}_2\text{C}_2]:[\mathbf{1}]$ ratios higher than ca. 50, and vice versa.

Therefore, the general rate law for the hydrogenation of diphenylacetylene promoted by complex **1** takes the form

$$v = v_1 + v_2 = -d[\text{Ph}_2\text{C}_2]/dt = \{k_a + k_b[\text{Ph}_2\text{C}_2]^{-1}\}[\mathbf{1}](P(\text{H}_2))$$

where $k_a = K_1k_2$ and $k_b = K_3K_4k_5$. This general rate law agrees well with all the experimental kinetic data, at any $[\text{Ph}_2\text{C}_2]:[\mathbf{1}]$ ratio.

Figure 1 clearly shows that *cis*-stilbene is the kinetic product and that it is progressively converted into *trans*-stilbene, indicating that there are two reactions competing for the same catalyst: the hydrogenation of the alkyne to a *cis*-alkene and the isomerization of the latter into a *trans*-alkene. However, we are sure that all our kinetic data correspond exclusively to the hydrogenation process, because no isomerization is observed in the first stages of the reaction (0–20 min), which are those in which we have carried out the kinetic studies.

Concerning the *cis*- to *trans*-alkene isomerization reaction, we have obtained no evidence that could support a possible mechanism. In fact, as far as we are aware, no reports concerning mechanisms for cluster-catalyzed *cis*- and *trans*-alkene isomerization reactions have ever been published. One big problem in studying these isomerization reactions is that the clusters that promote alkyne hydrogenation reactions do not promote any alkene isomerizations (actually, compounds **1** and **2** do not even react with *cis*-stilbene at 80 °C). In fact, it seems that short-lived catalytic intermediates of alkyne hydrogenation reactions are responsible for the alkene isomerization processes.

Concluding Remarks

This work presents a mechanism for the hydrogenation of diphenylacetylene promoted by complex **1** which involves only trinuclear cluster complexes, adding one example to the very few in which cluster catalysis has been supported both by the results of chemical reactions and by kinetic data.² This mechanism consists of two coupled catalytic cycles, one working preferably at low and the other preferably at high $[\text{substrate}]:[\text{catalyst}]$ ratios. In both cycles, the rate-determining step is the oxidative addition of hydrogen to the corresponding trinuclear cluster complex.

On the other hand, the results described in this article suggest that cluster compounds containing $\mu\text{-}\eta^1\text{:}\eta^2\text{-alkenyl}$ ligands should present an enhanced reactivity because they easily decoordinate the alkenyl C=C moiety to give coordinatively unsaturated derivatives containing terminal $\eta^1\text{-alkenyl}$ ligands. These kinds of "activated" compounds may have significance in stoichiometric and catalytic reactions; in fact, it has already been reported that the complex $[\text{Ru}_3(\mu_3\text{-anpy})(\mu\text{-}\eta^1\text{:}\eta^2\text{-PhC=CHPh})(\text{CO})_8]$ (Hanpy = 2-anilino-pyridine) codimerizes diphenylacetylene and ethylene under very mild conditions.^{9e}

Acknowledgment. This research was supported by the DGICYT (Project PB92-1007). A fellowship from the FICYT-Asturias (to A.L.) is also acknowledged.

Supplementary Material Available: Tables of bond distances and angles, torsion angles, anisotropic thermal parameters, and H-atom coordinates for $5\text{-CH}_2\text{Cl}_2$ (12 pages). Ordering information is given on any current masthead page.

OM940380V